Mechanisms Controlling the Sensitivity of Amperometric Biosensors in the Case of Substrate and Product Inhibition

Dainius Simelevicius and Romas Baronas
Faculty of Mathematics and Informatics
Vilnius University
Naugarduko 24, LT-03225 Vilnius, Lithuania
{*dainius.simelevicius, romas.baronas*}*@mif.vu.lt*

***Abstract*—Special case of amperometric biosensors is investigated in this paper. Processes of substrate as well as product inhibition take place during the operation of these biosensors. The operation of biosensors is modelled by employing non-stationary reaction-diffusion equations containing a non-linear term related to non-Michaelis-Menten kinetics. The equation system is solved numerically using finite difference technique. Apparent Michaelis constant is chosen as a good indicator of biosensor reliability. Its dependency on the substrate and product inhibition as well as the diffusion modulus and the Biot number was investigated.**

Keywords-modelling; simulation; apparent Michaelis constant; biosensor; inhibition.

I. Introduction

A biosensor is a device designed to measure concentration of some specific substance in a solution. Biosensors incorporate some biological material, usually an enzyme, thus its name. Enzymes are organic catalysts which catalyze very specific chemical reactions and do not infuence or participate in other reactions. This feature of enzymes is employed in biosensors for the recognition of particular chemicals in solutions [1]–[3]. Amperometric biosensors measure changes in the output current on the working electrode that occur due to the direct oxidation or reduction of products of the biochemical reaction. The output current is usually proportional to the concentration of an analyte (substrate) in a buffer solution. The concentration of an analyte is determined using the calibration curve prepared beforehand. Amperometric biosensors are known to be reliable, cheap and highly sensitive for environment monitoring, food analysis, clinical diagnostics, drug analysis and some other purposes [4]–[7].

Very frequently biosensors operate following the Michaelis-Menten kinetics scheme [2], [3],

$$\mathrm{E} + \mathrm{S} \underset{k_{-1}}{\overset{k_1}{\rightleftharpoons}} \mathrm{ES} \xrightarrow{k_2} \mathrm{E} + \mathrm{P}, \tag{1}$$

where E is the enzyme, S is the substrate, ES is the enzyme and substrate complex, and P is the reaction product, k_i is the reaction rate constant, $i = -1, 1, 2$. However, sometimes the kinetics of enzyme-catalysed reactions is much more complex. An inhibition, an activation, an allostery and other types of non-Michaelis-Menten kinetics are known for the diversity of enzymes [8]–[12].

This paper investigates the case when the standard scheme (1) is augmented with two more reactions

$$\mathrm{ES} + \mathrm{S} \underset{k_{-3}}{\overset{k_3}{\rightleftharpoons}} \mathrm{ESS}, \tag{2}$$

$$\mathrm{E} + \mathrm{P} \underset{k_{-4}}{\overset{k_4}{\rightleftharpoons}} \mathrm{EP}, \tag{3}$$

where ESS is a non-active complex with substrate molecule and EP is a non-active complex with product molecule, k_i is the reaction rate constant, $i = 3, -3, 4, -4$. The overall effect of reaction (2) is called substrate inhibition and the overall effect of reaction (3) is called product inhibition.

It is very important to investigate kinetic peculiarities of the biosensors [1]–[3]. In order to perform such investigation a model of a biosensor should be built [13], [14]. A thorough review on the modelling of the amperometric biosensors has been presented by Schulmeister [15] and more recently by Baronas et al. [16]. The same type of biosensors has been investigated in the paper by the same authors [17]. This paper enhances the results of investigation [17] and emphasizes on the sensitivity of biosensor at wide range of the inhibition constants, diffusion modulus and Biot values. Apparent Michaelis constant is used as a good indicator of biosensor sensitivity. A numerical simulation has been carried out using a finite difference technique [18], [19].

The rest of the paper is organised as follows: in Section II the mathematical model is described; Section III briefly describes the numerical model and the simulator; in Section IV we present results of numerical experiments; and, finally, the main conclusions are summarized in Section V.

II. Mathematical Model

Main parts of the amperometric biosensor are an electrode and a layer of enzyme applied on the electrode surface. The mathematical model consists of two layers: enzyme layer and diffusion layer. In enzyme layer enzymatic reaction and diffusion take place while in diffusion layer only diffusion

 ISBN: 978-1-61208-169-4

takes place. Outside the diffusion layer is the part of solution where the concentration of the analyte is kept constant.

Consideration that electrode and enzyme layer are symmetrical as well as consideration of homogeneous distribution of the immobilized enzyme in the enzyme membrane allows definition of one-dimensional-in-space mathematical model of the biosensor [15].

A. Governing Equations

By omitting the details of the catalysis mechanism, reaction scheme (1)–(3) may be generalized to the following form:

$$\mathrm{S} \xrightarrow{\mathrm{E}} \mathrm{P}. \tag{4}$$

Applying the quasi-steady-state approximation the rate of the reaction (4) may be expressed as follows [17]:

$$v(s_e, p_e) = \frac{V_{max} s_e}{k_M \left(1 + p_e/k_p\right) + s_e \left(1 + s_e/k_s\right)}, \tag{5}$$

where $s_e(x,t)$ and $p_e(x,t)$ are the molar concentrations of the substrate S and the product P in the enzyme layer, x and t stand for space and time, respectively, V_{max} is the maximal enzymatic rate, k_M is the Michaelis-Menten constant, k_s is the substrate inhibition rate, and k_p is the product inhibition rate [1], [2], [20]. These latter parameters are expressed as follows:

$$V_{max} = k_2 e_0 = k_2 (e_e + e_{es} + e_{ess} + e_{ep}), \tag{6a}$$

$$k_M = \frac{k_{-1} + k_2}{k_1}, \quad k_s = \frac{k_{-3}}{k_3}, \quad k_p = \frac{k_{-4}}{k_4}, \tag{6b}$$

where $e_e(x,t)$, $e_{es}(x,t)$, $e_{ess}(x,t)$ and $e_{ep}(x,t)$ are molar concentrations of the enzyme E, the ES complex, the ESS complex and the EP complex, respectively. e_0 is the total sum of the concentrations of all the enzyme forms, $e_0 = e_e + e_{es} + e_{ess} + e_{ep}$. e_0 is assumed to be constant in the entire enzyme layer.

Let $x = 0$ represents the electrode surface, $x = d_e$ is the boundary between the enzyme and the diffusion layers, and $x = d_e + d_d$ is the boundary between the diffusion layer and the bulk solution.

The governing equations for a chemical reaction network can be formulated by the law of mass action [1], [21]. Coupling of the enzyme-catalysed reaction in the enzyme layer with the one-dimensional-in-space diffusion, described by Fick's law, leads to the following equations of the reaction–diffusion type ($t > 0$):

$$\frac{\partial s_e}{\partial t} = D_{s_e} \frac{\partial^2 s_e}{\partial x^2} - v(s_e, p_e), \tag{7a}$$

$$\frac{\partial p_e}{\partial t} = D_{p_e} \frac{\partial^2 p_e}{\partial x^2} + v(s_e, p_e), \quad 0 < x < d_e, \tag{7b}$$

where d_e is the thickness of the enzyme layer, D_{s_e} and D_{p_e} are the diffusion coefficients of the substrate and the reaction product in the enzyme layer.

Outside the enzyme layer only the mass transport by diffusion of the substrate and the product takes place. We assume that the external mass transport obeys a finite diffusion regime,

$$\frac{\partial s_d}{\partial t} = D_{s_d} \frac{\partial^2 s_d}{\partial x^2}, \tag{8a}$$

$$\frac{\partial p_d}{\partial t} = D_{p_d} \frac{\partial^2 p_d}{\partial x^2}, \quad d_e < x < d_e + d_d, \quad t > 0, \tag{8b}$$

where $s_d(x,t)$ and $p_d(x,t)$ stand for concentrations of the substrate and the product in the diffusion layer, d_d is the thickness of the external diffusion layer, D_{s_d} and D_{p_d} are the diffusion coefficients in the diffusion layer.

B. Initial and Boundary Conditions

The biosensor operation starts when some substrate appears in the bulk solution ($t = 0$),

$$s_e(x,0) = 0, \quad p_e(x,0) = 0, \quad 0 \le x \le d_e, \tag{9a}$$

$$s_d(x,0) = 0, \quad p_d(x,0) = 0, \quad d_e \le x < d_e + d_d, \tag{9b}$$

$$s_d(d_e + d_d, 0) = s_0, \quad p_d(d_e + d_d, 0) = 0, \tag{9c}$$

where s_0 is the concentration of the analyte (substrate) in the bulk solution.

Due to the electrode polarization, concentration of the reaction product at the electrode surface ($x = 0$) is permanently reduced to zero [15],

$$p_e(0,t) = 0. \tag{10}$$

Since the substrate is not ionized, the substrate concentration flux on the electrode surface equals zero,

$$D_{s_e} \left.\frac{\partial s_e}{\partial x}\right|_{x=0} = 0. \tag{11}$$

The external diffusion layer ($d_e < x < d_e + d_d$) is treated as the Nernst diffusion layer [18]. According to the Nernst approach the layer of the thickness d_d remains unchanged with time. It is also assumed that away from it the solution is uniform in the concentration ($t > 0$),

$$s_d(d_e + d_d, t) = s_0, \tag{12a}$$

$$p_d(d_e + d_d, t) = 0. \tag{12b}$$

On the boundary between two regions having different diffusivities, the matching conditions have to be defined ($t > 0$),

$$D_{s_e} \left.\frac{\partial s_e}{\partial x}\right|_{x=d_e} = D_{s_d} \left.\frac{\partial s_d}{\partial x}\right|_{x=d_e}, \tag{13a}$$

$$s_e(d_e, t) = s_d(d_e, t), \tag{13b}$$

$$D_{p_e} \left.\frac{\partial p_e}{\partial x}\right|_{x=d_e} = D_{p_d} \left.\frac{\partial p_d}{\partial x}\right|_{x=d_e}, \tag{13c}$$

$$p_e(d_e, t) = p_d(d_e, t). \tag{13d}$$

 ISBN: 978-1-61208-169-4

According to these conditions, the substrate and the product concentration fluxes through the external diffusion layer are equal to the corresponding fluxes entering the surface of the enzyme layer. The concentrations of the substrate as well as the product from both layers are equal on the boundary between these layers.

C. Biosensor Response

The electric current is measured as a response of a biosensor in a physical experiment. The current depends on a flux of reaction product at an electrode surface. Thus the density i of the current at time t is proportional to the gradient of the product at the electrode surface, i.e., at the border $x = 0$, as described by Faraday's law,

$$i(t) = n_e F D_{p_e} \left. \frac{\partial p_e}{\partial x} \right|_{x=0}, \tag{14}$$

where n_e is a number of electrons involved in the electrochemical reaction, and F is Faraday's constant ($F = 96486\,\mathrm{C/mol}$) [2], [15].

Usually the steady-state current is used as a response of amperometric biosensor. However usage of steady-state current is not convenient when biosensor exhibits substrate and product inhibition, because steady-state current is directly proportional to s_0 only in part of the calibration curve [17]. The maximal biosensor current does not have this drawback,

$$i_{max} = \max_{t>0} i(t), \tag{15}$$

where i_{max} is the density of the maximal biosensor current.

D. Apparent Michaelis Constant

At the ideal conditions of the Michaelis-Menten model the rate of generalized reaction (4) is defined as follows:

$$v(s_0) = \frac{V_{max} s_0}{k_M + s_0}.$$

The maximal possible rate of generalized reaction (4) is equal

$$\lim_{s_0 \to \infty} v(s_0) = \lim_{s_0 \to \infty} \frac{V_{max} s_0}{k_M + s_0} = V_{max}$$

If the concentration s_0 is numerically equal to k_M then the rate of reaction (4) is equal to half the maximal possible reaction rate,

$$v(k_M) = \frac{V_{max} k_M}{k_M + k_M} = 0.5 V_{max}$$

If the biosensor would work at ideal Michaelis-Menten conditions, it would be possible to calculate k_M using the calibration curve $i_{max}(s_0)$, because $v(s_0)$ is proportional to $i_{max}(s_0)$,

$$V_{max} \sim \lim_{s_0 \to \infty} i_{max}(s_0), \quad 0.5 V_{max} \sim 0.5 \lim_{s_0 \to \infty} i_{max}(s_0).$$

When the Michaelis-Menten constant is calculated for the particular biosensor from the calibration curve it is called the apparent Michaelis constant k_{app},

$$k_{app} = \left\{ s_0^* : i_{max}(s_0^*) = 0.5 \lim_{s_0 \to \infty} i_{max}(s_0) \right\}. \tag{16}$$

Greater k_{app} value means longer range of substrate concentrations in which the calibration curve resembles a linear function. Whereas other parts of the curve are largely not suitable for the biosensor operation. This is the reason why k_{app} is an attractive parameter that helps to measure the sensitivity of biosensor.

Usually, for real biosensors $k_{app} \neq k_M$ [3]. Theoretical modelling has shown that under certain conditions k_{app} depends on the biosensor geometry [22]. It has been shown that k_{app} can be increased by the restriction of the substrate diffusivity [23]. This result can be easily applied for the biosensor improvement by covering the enzyme layer of a biosensor with a permeable membrane [23].

E. Limitations of Mathematical Model

The presented mathematical model is a simplified view of processes taking place during physical biosensor operation. Some processes are not reflected in the mathematical model. Physical experiments must obey some constraints in order to minimize the influence of those neglected processes.

The quasi-steady-state approximation used in the mathematical model neglects the fact that concentrations of enzyme forms (e_e, e_{es}, e_{ess} and e_{ep}) change at the beginning of a physical experiment. If the equilibrium between enzyme forms is reached fast enough this approximation is quite accurate though [20].

The enzyme layer should be of uniform thickness and the enzyme should be homogeneously distributed throughout this layer. This is an assumption leading to the construction of one-dimensional mathematical model. This approach is widely used and reliable, even though these conditions are not always satisfied because the enzyme layer often has more complicated geometry [16].

III. Numerical Simulation

The non-linearity of the governing equations prevents us from solving the initial boundary value problem (7)–(13) analytically, hence the numerical model is constructed and solved using finite difference technique [15], [18], [24]. An implicit finite difference scheme was built on a uniform discrete grid with 200 points in space direction [11], [17], [25], [26]. The simulator has been programmed by the authors in C language [27].

In the numerical simulation, the biosensor response time was assumed as the time when the change of the biosensor current over time remains very small during a relatively long term or when the biosensor current reaches local maximum

 ISBN: 978-1-61208-169-4

(which is the global function maximum too). A special dimensionless decay rate ε was used,

$$t_r = \min_{i(t)>0} \left\{ t : \frac{t}{i(t)} \frac{\mathrm{d}i(t)}{\mathrm{d}t} < \varepsilon \right\}, \quad i(t_r) \approx i_{max}, \qquad (17)$$

where t_r is the biosensor response time. The decay rate value $\varepsilon = 10^{-3}$ was used in the calculations.

In all numerical experiments the following values were kept constant:

$$\begin{aligned} &D_{s_e} = D_{p_e} = 100\,\mu\mathrm{m}^2/\mathrm{s}, \\ &D_{s_d} = 2D_{s_e}, \quad D_{p_d} = 2D_{p_e}, \\ &k_M = 0.01\,\mathrm{M}, \quad d_e = 10\,\mu\mathrm{m}, \quad n_e = 1. \end{aligned} \qquad (18)$$

IV. Results and Discussion

In order to conveniently analyse the simulation results, five dimensionless parameters were introduced:

$$\begin{aligned} K_{app} = \frac{k_{app}}{k_M}, \quad K_s = \frac{k_s}{k_M}, \quad K_p = \frac{k_p}{k_M}, \\ \alpha^2 = \frac{V_{max} d_e^2}{D_{S_e} k_M}, \quad Bi = \frac{d_e/D_{S_e}}{d_d/D_{S_d}} = \frac{D_{S_d} d_e}{D_{S_e} d_d}, \end{aligned} \qquad (19)$$

where K_{app}, K_s and K_p are the dimensionless apparent Michaelis constant, dimensionless substrate inhibition constant and dimensionless product inhibition constant, respectively, α^2 is called the diffusion mudulus and Bi is the Biot number.

A. Apparent Michaelis Constant vs. Substrate and Product Inhibition

The dependence of the apparent Michaelis constant on the substrate and product inhibition rates were investigated in a wide range of inhibition constant values ($K_s, K_p \in [10^{-4}..10^{4}]$). The dependence on the substrate inhibition was investigated at three fixed rates of the product inhibition: no product inhibition ($K_p \to \infty$, curve 1), moderate product inhibition ($K_p = 1$, curve 2) and high product inhibition ($K_p = 0.01$, curve 3). In the case of no product inhibition, the reaction scheme (1)–(3) reduces to scheme (1), (2). The dependence on the product inhibition was investigated at three fixed rates of the substrate inhibition: no substrate inhibition ($K_s \to \infty$, curve 4), moderate substrate inhibition ($K_s = 1$, curve 5) and high substrate inhibition ($K_s = 0.01$, curve 6). In the case of no substrate inhibition, the reaction scheme (1)–(3) reduces to scheme (1), (3). Other parameters were kept as follows: $\alpha^2 = 0.01$, $Bi = 1/15 (d_d = 300\,\mu\mathrm{m})$. The results of the numerical simulation are depicted in Figure 1.

The apparent Michaelis constant does not dependent on the product inhibition rate at the very wide range of product inhibition constant values ($K_p \in [10^{-2}..10^{4}]$). However at extremely high rates of product inhibition ($K_p \in [10^{-4}..10^{-2}]$) and no substrate inhibition (curve 4), the apparent Michaelis constant is dependent on product inhibition rate change. K_{app} is inversely proportional to the

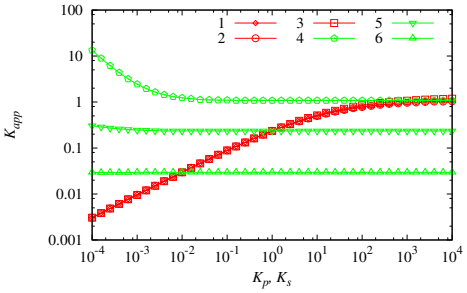

Figure 1. The dependence of the apparent Michaelis constant K_{app} on substrate (1, 2, 3) and product (4, 5, 6) inhibition constants K_s and K_p, respectively.

K_p. However, the presence of substrate inhibition eliminates the effect. In the case of a moderate substrate inhibition ($K_s = 1$, curve 5) the infuence is barely observable and in the case of high substrate inhibition ($K_s = 0.01$, curve 6) the effect vanishes.

As one can see from the Figure 1 (curves 1, 2 and 3) the apparent Michaelis constant continuously and non-linearly increases with an increase in K_s. At low rates of the substrate inhibition the slope of curves starts to decrease as the function approaches the maximal value of K_{app} at these particular biosensor parameters. As moderate and low product inhibition rates do not influence K_{app} value, all three curves depicting the dependence on K_s almost entirely coincide. However at low substrate inhibition values (high K_s values), the curve 3 representing high product inhibition ($K_p = 0.01$) slightly separates from curves 1, 2 representing no product inhibition and low product inhibition ($K_p = 1$). This is the same positive effect of the product inhibition that is clearly observed on curve 4.

After examination of Figure 1 we can conclude that the substrate and product inhibitions have opposite effects on the apparent Michaelis constant. However, the infuence of the substrate inhibition is evident at the very wide range of substrate inhibition values, while infuence of the product inhibition is evident only at the very high rates of product inhibition and when this effect is not masked by the opposite effect of substrate inhibition.

B. Apparent Michaelis Constant vs. Diffusion Modulus

To investigate the dependence of the apparent Michaelis constant on the diffusion modulus α^2, K_{app} was calculated simulating biosensor action at three values of the substrate inhibition: high substrate inhibition ($K_s = 0.01$), moderate substrate inhibition ($K_s = 0.1$) and low substrate inhibition ($K_s = 1$) as well as at three values of the Biot number: $Bi = 0.01$, $Bi = 1$ and $Bi = 100$. Calculation results are depicted in Figure 2.

As it is evident from Figure 2, the apparent Michaelis constant is directly proportional to the diffusion modulus

 ISBN: 978-1-61208-169-4

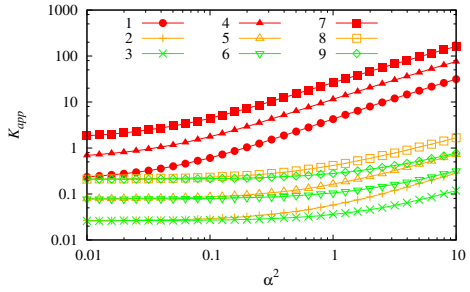

Figure 2. The dependence of the apparent Michaelis constant K_{app} on the diffusion modulus α^2 at three rates of the substrate inhibition (K_s): 0.01 (1, 2, 3), 0.1 (4, 5, 6), 1 (7, 8, 9) and at three rates of the Biot number Bi: 0.01 (1, 4, 7), 1 (2, 5, 8), 100 (3, 6, 9), $K_p = 0.1$.

α^2, not in a whole range of α^2 though. The value of Biot number determines the point at which the diffusion modulus starts to infuence the K_{app} value. As one can see from Figure 2, when the Biot number is low (curves 1, 4 and 7) the diffusion modulus starts infuencing the K_{app} at the values as low as $\alpha^2 = 0.01$, when the Biot number is moderate and high (curves 2, 5, 8 and 3, 6, 9, respectively) the diffusion modulus starts infuencing the K_{app} at the values of $\alpha^2 = 0.1$. By comparing the steepness of curves we can deduce that the Biot number also determines the sensitivity of the K_{app} to the α^2. The curves 1, 4 and 7 that represent a small value of the Biot number ($Bi = 0.01$) are steeper than curves 2, 5, 8 that represent a moderate Biot number value ($Bi = 1$) which are steeper than curves 3, 6, 9 that represent a high Biot number value ($Bi = 100$) accordingly. The more steep the curve is, the more sensitive is the apparent Michaelis constant to the diffusion modulus.

The substrate inhibition rate influences the apparent Michaelis constant in the whole investigated range of the diffusion modulus α^2 as well as at all investigated values of the Biot number. K_{app} is directly proportional to the substrate inhibition constant K_s.

The apparent Michaelis constant is inversely proportional to the Biot number. The values of K_{app} are higher at low Biot number values $Bi = 0.01$ (curves 1, 4, 7) than at high and moderate Biot number values $Bi = 100$ (curves 3, 6, 9) and $Bi = 1$ (curves 2, 5, 8), respectively. However when the Biot number is moderate and high and at lower values of diffusion modulus, the Biot number does not influence K_{app}.

C. Apparent Michaelis Constant vs. Biot Number

Figure 3 represents the effect of the Biot number on the apparent Michaelis constant. One can see in Figure 3, that K_{app} is a monotonous descreasing function of Bi. However, at higher values of Bi the function reaches the steady-state and K_{app} value sets in. The range of Bi where the function $K_{app}(Bi)$ is at steady-state depends on the diffusion modulus though. When the diffusion modulus is low $\alpha^2 = 0.1$ (curves 1, 4), the range of steady-state is wide ($Bi \in [1..100]$), when diffusion modulus is moderate and high $\alpha^2 = 1$ and $\alpha^2 = 10$, respectively, the range of steady-state is narrower.

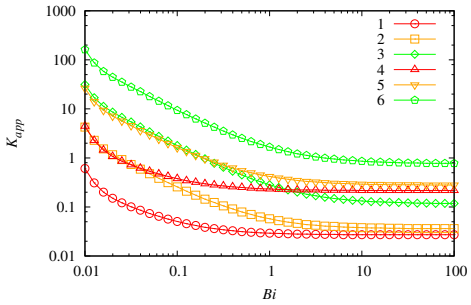

Figure 3. The dependence of the apparent Michaelis constant K_{app} on the Biot number Bi at two rates of the substrate inhibition (K_s): 0.01 (1, 2, 3), 1 (4, 5, 6) and at three rates of the diffusion modulus α^2: 0.1 (1, 4), 1 (2, 5), 10 (3, 6), $K_p = 0.1$.

V. Conclusion

The mathematical model (7)–(13) of the amperometric biosensor with the substrate and product inhibition can be successfully used to investigate the behaviour of the biosensor response at various sets of parameters. The model can be used as a tool to optimize the biosensor configuration prior to the experimental stage.

The substrate inhibition decreases the value of the apparent Michaelis constant, hence designers of biosensors should avoid the substrate inhibition if possible. Whereas the product inhibition may increase the value of the apparent Michaelis constant and make the biosensor more attractive (Figure 1).

If the substrate inhibition is unavoidable and the apparent Michaelis constant is low, the biosensor can be improved by increasing the diffusion modulus α^2 (Figure 2). Practically this can be achieved be increasing the enzyme layer thickness d_e or by increasing enzyme concentration e_0.

Another possibility to improve the biosensor is to increase the external diffusion layer thickness d_d or decrease the substrate diffusivity D_{S_d}. This can be achieved be decreasing the intensity of solution stirring or by covering the enzyme layer of a biosensor with a permeable membrane which would decrease the substrate diffusivity. In worst cases this method may at least move the value of apparent Michaelis constant close to the Michaelis-Menten constant. In the best cases, apparent Michaelis constant may overwhelm the Michaelis-Menten constant by a few orders of magnitude (Figure 3).

Acknowledgment

This research was funded by the European Social Fund under Measure VP1-3.1-ŠMM-07-K "Support to Research

of Scientists and Other Researchers (Global Grant)", Project "Developing computational techniques, algorithms and tools for efficient simulation and optimization of biosensors of complex geometry".

REFERENCES

[1] H. Gutfreund, *Kinetics for the Life Sciences*. Cambridge: Cambridge University Press, 1995.

[2] F. W. Scheller and F. Schubert, *Biosensors*. Amsterdam: Elsevier Science, 1992.

[3] A. P. F. Turner, I. Karube, and G. S. Wilson, *Biosensors: Fundamentals and Applications*. Oxford: Oxford University Press, 1990.

[4] J. F. Liang, Y. T. Li, and V. C. Yang, "Biomedical application of immobilized enzymes," *Journal of Pharmaceutical Sciences*, vol. 89, no. 8, pp. 979–990, 2000.

[5] K. R. Rogers, "Biosensors for environmental applications," *Biosensors and Bioelectronics*, vol. 10, no. 6–7, pp. 533–541, 1995.

[6] F. W. Scheller, F. Schubert, and J. Fedrowitz, *Frontiers in Biosensorics II. Practical Applications*. Basel: Birkhäuser, 1997, vol. 2.

[7] D. Yu, B. Blankert, J. C. Vire, and J. M. Kauffmann, "Biosensors in drug discovery and drug analysis," *Analytical Letters*, vol. 38, no. 11, pp. 1687–1701, 2005.

[8] A. Chaubey and B. D. Malhotra, "Mediated biosensors," *Biosensors and Bioelectronics*, vol. 17, no. 6–7, pp. 441–456, 2002.

[9] A. Cornish-Bowden, *Fundamentals of Enzyme Kinetics*, 3rd ed. London: Portland Press, 2004.

[10] N. C. of the International Union of Biochemistry, "Symbolism and terminology in enzyme kinetics," *Biochemical Journal*, vol. 213, no. 3, pp. 561–571, 1983.

[11] R. Baronas, F. Ivanauskas, and J. Kulys, "The effect of diffusion limitations on the response of amperometric biosensors with substrate cyclic conversion," *Journal of Mathematical Chemistry*, vol. 35, no. 3, pp. 199–213, 2004.

[12] J. Kulys, "Biosensor response at mixed enzyme kinetics and external diffusion limitation in case of substrate inhibition," *Nonlinear Analysis: Modelling and Control*, vol. 11, no. 4, pp. 385–392, 2006.

[13] J. R. D. Corcuera, R. Cavalieri, J. Powers, and J. Tang, "Amperometric enzyme biosensor optimization using mathematical modeling," in *Proceedings of the 2004 ASAE / Csae Annual International Meeting*. Ottawa, Ontario: American Society of Agricultural Engineers, 2004, p. 47030.

[14] L. S. Ferreira, M. B. D. Souza, J. O. Trierweiler, O. Broxtermann, R. O. M. Folly, and B. Hitzmann, "Aspects concerning the use of biosensors for process control: experimental and simulation investigations," *Computers and Chemical Engineering*, vol. 27, no. 8, pp. 1165–1173, 2003.

[15] T. Schulmeister, "Mathematical modelling of the dynamic behaviour of amperometric enzyme electrodes," *Selective Electrode Reviews*, vol. 12, pp. 203–260, 1990.

[16] R. Baronas, F. Ivanauskas, and J. Kulys, *Mathematical Modeling of Biosensors*, ser. Springer Series on Chemical Sensors and Biosensors, G. Urban, Ed. Dordrecht: Springer, 2010, vol. 9.

[17] D. Šimelevičius and R. Baronas, "Computational modelling of amperometric biosensors in the case of substrate and product inhibition," *Journal of Mathematical Chemistry*, vol. 47, no. 1, pp. 430–445, 2010.

[18] D. Britz, *Digital Simulation in Electrochemistry*, 3rd ed., ser. Lecture Notes in Physics. Berlin: Springer, 2005, vol. 666.

[19] A. A. Samarskii, *The Theory of Difference Schemes*. New York: Marcel Dekker, 2001.

[20] B. Li, Y. Shen, and B. Li, "Quasi-steady state laws in enzyme kinetics," *The Journal of Physical Chemistry A*, vol. 112, no. 11, pp. 2311–2321, 2008.

[21] P. N. Bartlett and R. G. Whitaker, "Electrochemical imobilisation of enzymes: Part 1. theory," *Journal of Electroanalytical Chemistry*, vol. 224, no. 1–2, pp. 27–35, 1987.

[22] F. Ivanauskas, I. Kaunietis, V. Laurinavičius, J. Razumienė, and R. Šimkus, "Apparent Michaelis constant of the enzyme modified porous electrode," *Journal of Mathematical Chemistry*, vol. 43, no. 4, pp. 1516–1526, 2008.

[23] O. Štikonienė, F. Ivanauskas, and V. Laurinavičius, "The influence of external factors on the operational stability of the biosensor response," *Talanta*, vol. 81, no. 4-5, pp. 1245–1249, 2010.

[24] J. P. Kernevez, *Enzyme Mathematics. Studies in Mathematics and its Applications*. Amsterdam: Elsevier Science, 1980.

[25] R. Baronas, J. Kulys, and F. Ivanauskas, "Computational modeling of biosensors with perforated and selective membranes," *Journal of Mathematical Chemistry*, vol. 39, no. 2, pp. 345–362, 2006.

[26] R. Baronas, F. Ivanauskas, and J. Kulys, "Computational modeling of the behaviour of potentiometric membrane biosensors," *Journal of Mathematical Chemistry*, vol. 42, no. 3, pp. 321–336, 2007.

[27] W. H. Press, S. A. Teukolsky, W. T. Vetterling, and B. P. Flannery, *Numerical Recipes in C: The Art of Scientific Computing*, 2nd ed. Cambridge: Cambridge University Press, 1992.

 ISBN: 978-1-61208-169-4